Voltage Stability Analysis and Online Monitoring Method Based on Fixed-Point Principle and Spectrum Calculation

Fan LI[1,*], Fang-zong WANG[1], Xue-tao YANG[2] and Dun-wen SONG[2]

[1]China Three Gorges University, Yichang 443002, Hubei Province, China

[2]China Electric Power Research Institute, Haidian District, Beijing 100192, China

*Corresponding author

Keywords: Voltage stability, Thévenin equivalent, Fixed-point principle, Spectral analysis method, Cholesky decomposition.

Abstract. Accurate voltage stability analysis and online monitoring are essential to ensure a secure operation of the power system. To this end, researchers have proposed a variety of voltage stability indicators and analysis methods, of which, the voltage stability analysis method based on Thévenin equivalent has been widely concerned. However, due to the lack of simple and effective online identification method for Thévenin equivalent parameters, this method is still difficult to apply online. In this paper, the fixed point principle is applied to voltage stability analysis, and a new voltage stability criterion is proposed. Furthermore, in order to determine the physical correspondence between the spectral distribution and each specific load, this paper derives a numerical method for quickly estimating the spectral distribution. Based on the above, this paper proposes a new online analysis and monitoring method for voltage stability. The proposed method was tested on 3-machines and 10-bus system, and compared with the voltage stability analysis method based on Thévenin equivalent. The results show that the proposed method in this paper is effective.

Introduction

Since the 1990s, great progress has been made in the study of voltage stability in power systems. So far, researchers have proposed a variety of voltage stability indicators and analysis methods[1-9], of which, the voltage stability analysis method based on Thévenin equivalent has been widely concerned[10-13].

Thévenin equivalent is an important concept in linear circuit theory, which has wide application value. For time-varying non-linear circuits, in principle, at any time section, the non-linear circuit can be simplified to a Thévenin equivalent circuit of a node. Therefore, the voltage stability analysis method based on Thévenin equivalence not only has the advantages of clear physical concept, simple model, and can clearly characterize the voltage stability of the power system, but also has good practical application prospects. In 1999, Khoi Vu and other scholars took the lead in putting forward the online identification of Thévenin equivalent parameters and voltage stability monitoring method based on local measurement[6]. Since then, scholars in various countries have continuously improved and improved on this basis and put forward various improved Thévenin equivalent parameter calculation models and methods[12]. However, existing methods for identifying Thévenin equivalent parameters based on in-situ measurements are based on the assumption that the Thévenin equivalent parameters between two adjacent state points or time sections remain unchanged. Obviously, this assumption is not strictly valid, because every operating point of the system should correspond to a unique set of deterministic Thévenin equivalent parameters. Therefore, how to accurately track and estimate the dynamic Thévenin equivalent parameters is still an unsolved problem[7-9].

In order to avoid the above problems, the paper [11] proposes a method of tracking Thévenin equivalent parameters based on time domain simulation and develops a corresponding program for calculating Thévenin equivalent parameters in FDS system[12]. In theory, this method of calculating Thévenin's equivalent parameters based on time domain simulation is accurate and reliable, but the results of literature [14] show that different Thévenin's equivalent methods can get different equivalent parameters. Therefore, the calculation of Thévenin's equivalent parameters is uncertain, that is, multivalued problem. In addition, Thévenin equivalent parameter tracking method based on time domain simulation needs to consider the global network equation, and the admittance matrix of the system needs to be modified and the corresponding network equation is solved at each time. The calculation amount is large, so it is difficult to apply it online.

In order to avoid the technical problem of accurate calculation of Thévenin's equivalent parameters[7,14], a channel component transforms (CCT) method is proposed in reference [8]. The core idea of CCT method is to decouple the coupled network equations into multiple independent channels by eigenvalue decomposition, and each channel is similar to a Thévenin equivalent circuit. CCT method provides a new ideal for on-line analysis and monitoring of voltage stability. However, the CCT method needs eigenvalue decomposition. For a large-scale power system, the corresponding eigenvalue decomposition is time-consuming. Another key problem is that the existing eigenvalue decomposition method can't directly determine the physical correspondence between the eigenvalue and the load node, nor can it directly determine the physical correspondence between the channel and the load. In order to correlate the analysis results of voltage stability based on channel components with specific loads, reference [8] adopts the identification method based on contribution index.

In this paper, the fixed-point principle[15] is used to illustrate the voltage stability problem. Its core idea is: if the system has a unique fixed-point in the voltage metric space, the system is voltage stability. Therefore, according to the basic fixed point theorem, i. e. the compression mapping principle, the voltage stability of the power system can be analyzed and judged by the spectral analysis method. In order to determine the physical correspondence between the eigenvalue distribution and the specific loads, a new method for calculating the spectral distribution of the admittance matrix of shrinking nodes is presented in this paper. Generally speaking, the proposed method of voltage stability analysis and calculation has the advantages of less calculation and faster calculation speed and can be used for on-line monitoring of voltage stability.

Voltage Stability Analysis Method Based on Fixed Point Principle

The Theoretical Basis

Although accurate tracking and estimation of Thévenin equivalent parameters is still a technical problem, the voltage stability analysis method based on Thévenin equivalent has been widely recognized by researchers. Therefore, in order to facilitate understanding, this paper starts with the basic Thévenin equivalent circuit and then elaborates the voltage stability analysis method based on the fixed point principle.

As shown in Figure. 1, for an actual power system, an "observation" of the system from a load bus at any time section can be regarded as a two-node system in which a voltage source supplies power to the studied load bus through an impedance, which is the Thévenin equivalent.

In Figure. 1, $\boldsymbol{E}_s(t)$ and $\boldsymbol{Z}_s(t)$ are Thévenin's equivalent internal potential and equivalent impedance at t time, $\boldsymbol{v}_k(t)$ and $\boldsymbol{i}_k(t)$ are load bus voltage and current at corresponding time, respectively, and load power is $\boldsymbol{S}_k(t) = p_k(t) + \mathrm{j}q_k(t)$, and load's equivalent impedance is recorded as $\boldsymbol{Z}_k(t)$.

(a) Original power system (b) Thevenin equivalent system

Figure 1. Thévenin equivalent illustration

On the premise that Thévenin's equivalent parameters are accurate and effective, the voltage stability of Thevenin's equivalent system can be analyzed by "impedance mode criterion". That is, $|\boldsymbol{Z}_s| < |\boldsymbol{Z}_k|$, the voltage of the load node is stable; otherwise, the voltage is unstable.

For the Thévenin equivalent circuit shown in Figure 1, there are:

$$\boldsymbol{v}_k = \boldsymbol{E}_s - \boldsymbol{i}_k(\boldsymbol{v}_k)\boldsymbol{Z}_s \triangleq \boldsymbol{f}(\boldsymbol{v}_k) \quad (1)$$

Where, $\boldsymbol{i}_k(\boldsymbol{v}_k)$ denotes that it is a function of the voltage state variable $\boldsymbol{v}_k$. Obviously, when Thévenin's equivalent parameter is fixed, $\boldsymbol{f}(\boldsymbol{v}_k)$ is the so-called self-mapping function about $\boldsymbol{v}_k$.

Based on equation (1), the problem of voltage stability can be described as follows: if the load node voltage $\boldsymbol{v}_k$ can be maintained at a certain equilibrium point in the case of disturbance, the node voltage $\boldsymbol{v}_k$ will be stable; if the load node voltage $\boldsymbol{v}_k$ cannot be maintained at a certain equilibrium point in the case of disturbance, the voltage $\boldsymbol{v}_k$ will be unstable.

According to the fixed point theory, for the general nonlinear self-mapping equation $\boldsymbol{x} = \boldsymbol{f}(\boldsymbol{x})$, $\boldsymbol{x} \in \mathrm{R}^n$, the so-called fixed point is the equilibrium point $\boldsymbol{x}_s = \boldsymbol{f}(\boldsymbol{x}_s)$ under perturbation. Therefore, based on the above description of voltage stability, we can naturally apply the fixed point principle to study voltage stability: if the non-linear equation (1) has a unique fixed point in a specific interval, the system will be voltage stability. In fact, the fixed point theory mainly studies the existence, number, nature and calculation method of fixed points. Therefore, the fixed point theory is the main theoretical basis for studying the existence, uniqueness and iterative solution of various equations.

There are mainly Banach fixed-point theorem and Brouwer fixed-point theorem for fixed-point theorem[14]. In this paper, Banach fixed point theorem is used to study voltage stability. To avoid complication, the theorem can be summarized as follows.

Banach Fixed Point Theorem: Let $\boldsymbol{f}(\boldsymbol{x})$ be a mapping from space $[a \quad b]$ to itself, $\boldsymbol{x},\boldsymbol{y} \in [a \quad b]$ and $\boldsymbol{x} \neq \boldsymbol{y}$. If there is $|\boldsymbol{f}(\boldsymbol{x}) - \boldsymbol{f}(\boldsymbol{y})| \leq \mu|\boldsymbol{x} - \boldsymbol{y}|$, $\mu < 1$, then for an initial value $\boldsymbol{x}_0 \in [a \quad b]$, the series $\boldsymbol{x}_{n+1} = \boldsymbol{f}(\boldsymbol{x}_n)$ generated by iteration $\{\boldsymbol{x}_n\}$ must converge and have $\lim_{n\to\infty} \boldsymbol{x}_n = \boldsymbol{x}_s = f(\boldsymbol{x}_s)$, that is, $\boldsymbol{x}_s$ is the only fixed point of self-mapping $\boldsymbol{x} = \boldsymbol{f}(\boldsymbol{x})$ on the interval $[a \quad b]$.

In the above expression: $|\bullet|$ is Banach spatial measure, can simply be understood as the Euclidean vector norm. $\mu < 1$, so $|\boldsymbol{f}(\boldsymbol{x}) - \boldsymbol{f}(\boldsymbol{y})| \leq \mu|\boldsymbol{x} - \boldsymbol{y}|$ is a contractive mapping. Therefore, Banach fixed point theorem, also known as the contraction mapping principle, is an important tool of metric space theory. It provides a strictly theoretical basis for the existence and uniqueness of fixed points of self-mapping in metric space, and provides a constructive method for finding these fixed points.

The above contractive mapping can be expressed in Euclidean space as follows:

$$\left\| \frac{\partial \boldsymbol{f}(\boldsymbol{x})}{\partial \boldsymbol{x}} \right\| = \mu < 1 \quad (2)$$

In the above formula: $\|\bullet\|$ represents the norm of a matrix, which can be specified by column and norm, row and norm or spectral norm (denoted as $\|\bullet\|_2 = \rho(\bullet)$). Thus, the principle of contractive mapping can be explained by a simple numerical iteration method: if formula (2) holds, the following iteration method.

$$\boldsymbol{x}_{n+1} = \boldsymbol{f}(\boldsymbol{x}_n), \quad \boldsymbol{x}_0 \in [a \quad b] \quad (3)$$

It will converge to the only equilibrium point $\boldsymbol{x}_s = f(\boldsymbol{x}_s)$. The scheme (3) is a well-known fixed point iteration method, and the equation (2) is a sufficient condition for the convergence of the fixed point iteration method.

According to equation (1), there are:

$$\frac{\partial \boldsymbol{f}(\boldsymbol{v}_k)}{\partial \boldsymbol{v}_k} = -\frac{\partial \boldsymbol{i}_k(\boldsymbol{v}_k)}{\partial \boldsymbol{v}_k}\boldsymbol{Z}_s \quad (4)$$

Hence,

$$\left\|\frac{\partial \boldsymbol{f}(\boldsymbol{v}_k)}{\partial \boldsymbol{v}_k}\right\| = \left\|\frac{\boldsymbol{Z}_s}{\boldsymbol{Z}_k}\right\| = \frac{|\boldsymbol{Z}_s|}{|\boldsymbol{Z}_k|} \tag{5}$$

Based on the above fixed point theorem, we can see that if there is a constant $|\boldsymbol{Z}_s|/|\boldsymbol{Z}_k| < 1$ in a certain interval, then equation (1) has a unique fixed point in that interval, that is:

$$\boldsymbol{v}_k = \frac{\boldsymbol{Z}_k}{\boldsymbol{Z}_s + \boldsymbol{Z}_k}\boldsymbol{E}_s \tag{6}$$

Based on the actual power system, the above "certain interval" can be defined as: $|\boldsymbol{v}_k| \in [v_{min} \quad |\boldsymbol{E}_s|]$, where, v_{min} represents the limit of voltage stability set in engineering practice (China usually set to 0.75pu).

Generally speaking, according to the fixed point principle, if there is constant $|\boldsymbol{Z}_s| < |\boldsymbol{Z}_k|$ in interval $|\boldsymbol{v}_k| \in [v_{min} \quad |\boldsymbol{E}_s|]$, the load node voltage $\boldsymbol{v}_k$ will be stable; otherwise, the load node voltage will be unstable. Obviously, the voltage stability criterion based on the fixed point theorem is consistent with the so-called "impedance mode criterion".

Basic Criteria for Voltage Stability Analysis

In this section, the voltage stability analysis method of power system based on fixed point principle is introduced.

As we all know, for a certain time section, the nodal network equation of the power grid is:

$$\boldsymbol{YU} = \boldsymbol{I} \tag{7}$$

Where, $\boldsymbol{Y}$ is the node admittance matrix of the network; $\boldsymbol{U}(t)$ is the node voltage column vector of the time section; $\boldsymbol{I}(t)$ is the node injection current column vector. According to the classification of network nodes, the above network equation can be further expressed as:

$$\begin{bmatrix} \boldsymbol{Y}_{GG} & \boldsymbol{Y}_{GL} & \boldsymbol{Y}_{GN} \\ \boldsymbol{Y}_{LG} & \boldsymbol{Y}_{LL} & \boldsymbol{Y}_{LN} \\ \boldsymbol{Y}_{NG} & \boldsymbol{Y}_{NL} & \boldsymbol{Y}_{NN} \end{bmatrix} \begin{bmatrix} \boldsymbol{E}_G \\ \boldsymbol{V}_L \\ \boldsymbol{U}_N \end{bmatrix} = \begin{bmatrix} \boldsymbol{I}_G \\ -\boldsymbol{I}_L \\ \boldsymbol{0} \end{bmatrix} \tag{8}$$

Where, $\boldsymbol{E}_G$、$\boldsymbol{I}_G$ represent the generator terminal voltage column vector and generator injection current column vector respectively; $\boldsymbol{V}_L$、$\boldsymbol{I}_L$ represents the load node voltage column vector and load current column vector respectively; $\boldsymbol{U}_N$ is the contact node voltage column vector, so-called contact node is the network node that neither generators nor loads are connected, and the injection current of such node is **0**.

From equation (8),

$$\boldsymbol{V}_L = \boldsymbol{CE}_G - \boldsymbol{y}_L^{-1}\boldsymbol{I}_L \tag{9}$$

Where,

$$\boldsymbol{C} \triangleq \boldsymbol{y}_L^{-1}\boldsymbol{y}_G \tag{10}$$

$$\boldsymbol{y}_G \triangleq \boldsymbol{Y}_{LN}\boldsymbol{Y}_{NN}^{-1}\boldsymbol{Y}_{NG} - \boldsymbol{Y}_{LG} \tag{11}$$

$$\boldsymbol{y}_L \triangleq \boldsymbol{Y}_{LL} - \boldsymbol{Y}_{LN}\boldsymbol{Y}_{NN}^{-1}\boldsymbol{Y}_{NL} \tag{12}$$

When the network topology is fixed, both $\boldsymbol{C}$ and $\boldsymbol{y}_L$ in the above expressions are stationary matrices. For a certain time section, the generator terminal voltage column vector $\boldsymbol{E}_G$ will be determined; when a load of each node is fixed, the load node current $\boldsymbol{I}_L$ is a function of the joint point voltage. Thus, equation (9) can be further expressed in the following form:

$$\boldsymbol{V}_L = \boldsymbol{C}\boldsymbol{E}_G - \boldsymbol{y}_L^{-1}\boldsymbol{I}_L(\boldsymbol{V}_L) \triangleq \boldsymbol{F}(\boldsymbol{V}_L) \tag{13}$$

Hence,

$$\frac{\partial \boldsymbol{F}(\boldsymbol{V}_L)}{\partial \boldsymbol{V}_L} = -\boldsymbol{y}_L^{-1}\frac{\partial \boldsymbol{I}_L(\boldsymbol{V}_L)}{\partial \boldsymbol{V}_L} \tag{14}$$

Where,

$$\boldsymbol{y}_L \triangleq \begin{bmatrix} \boldsymbol{B}_L & \boldsymbol{G}_L \\ \boldsymbol{G}_L & -\boldsymbol{B}_L \end{bmatrix} \tag{15}$$

Then,

$$\frac{\partial \boldsymbol{I}_L(\boldsymbol{V}_L)}{\partial \boldsymbol{V}_L} \triangleq \boldsymbol{Y}_{eq} = \begin{bmatrix} -\boldsymbol{\beta} & \boldsymbol{\alpha} \\ \boldsymbol{\alpha} & \boldsymbol{\beta} \end{bmatrix} \tag{16}$$

$$\boldsymbol{\alpha} = diag\left(\alpha_k\right), \quad \alpha_k \triangleq p_k / v_k^2 \tag{17}$$

$$\boldsymbol{\beta} = diag\left(\beta_k\right), \quad \beta_k \triangleq q_k / v_k^2 \tag{18}$$

Where, p_k and q_k are the active and reactive power of the k load ($k \in (1,\ m)$), and v_k is the node voltage amplitude.

Based on the above deduction, there is:

$$\left\| \frac{\partial \boldsymbol{F}(\boldsymbol{V}_L)}{\partial \boldsymbol{V}_L} \right\|_2 \triangleq \rho\left(\boldsymbol{y}_L^{-1}\boldsymbol{Y}_{eq}\right) \tag{19}$$

According to the fixed point theorem, if:

$$\rho(\boldsymbol{y}_L^{-1}\boldsymbol{Y}_{eq})<1 \tag{20}$$

Then equation (13) has a unique fixed point at the time section and is therefore voltage stable. Equation (20) is the criterion to judge whether the voltage of the power system is stable or not.

Using existing software tools, $\rho(\boldsymbol{y}_L^{-1}\boldsymbol{Y}_{eq}(t))$ can be calculated accurately. Therefore, it is feasible and strict to use the above criterion (20) to judge the voltage stability of a large-scale power system.

Voltage Stability Analysis Based Method on Spectrum Calculation

It's easy to understand if only a simple calculation of $\rho(\boldsymbol{y}_L^{-1}\boldsymbol{Y}_{eq})$, it can determine whether the entire system voltage stability, but can not analyze each load voltage stability margin or unstable degree. In order to analyze the voltage stability of each specific load, it is necessary not only to calculate or estimate the spectral distribution of matrix $\boldsymbol{y}_L^{-1}\boldsymbol{Y}_{eq}$, i.e. the eigenvalue distribution, but also to determine the physical correspondence between the eigenvalue distribution and the specific load.

It is easy to understand that $\boldsymbol{y}_L$ is a contractive admittance matrix. In order to calculate the spectral distribution of $\boldsymbol{y}_L$, the following lemmas are introduced.

Lemma 1 In the power system, both a real part $\boldsymbol{G}$ and imaginary part $-\boldsymbol{B}$ of the nodal admittance matrix are real symmetric positive definite matrices.

Lemma 2 Supposes that matrix $\boldsymbol{A} \triangleq \left[a_{ij}\right] \in \mathrm{R}^n$ is a lower triangular matrix or an upper triangular matrix. If the elements $a_{ii} \neq 0$, $i \in (1,\ n)$ on the diagonal line of the matrix are completely different from each other, then the matrix can be diagonalized, and its characteristic value is the element on the diagonal line, that is, $\lambda_k(\boldsymbol{A}) = a_{kk}$, $k \in (1,\ n)$ [16].

Based on **Lemma 1**, it is known that both real part $\boldsymbol{G}_L$ and imaginary part $-\boldsymbol{B}_L$ of the contractive admittance matrix $\boldsymbol{y}_L$ are real symmetric positive definite matrices. Therefore, they have the following Cholesky decomposition:

$$-\boldsymbol{B}_L = \boldsymbol{L}_1\boldsymbol{L}_1^{\mathrm{T}},\ \boldsymbol{L}_1 \triangleq \left[b_{ij}\right] \tag{21}$$

$$\boldsymbol{G}_L = \boldsymbol{L}_2\boldsymbol{L}_2^{\mathrm{T}},\ \boldsymbol{L}_2 \triangleq \left[g_{ij}\right] \tag{22}$$

In the above expressions, both $\boldsymbol{L}_1$ and $\boldsymbol{L}_2$ are lower triangular matrices, and the elements on the diagonal lines are greater than 0.

By using the Cholesky decomposition, there is:

$$\boldsymbol{y}_L = \boldsymbol{Q}\begin{bmatrix} -\boldsymbol{I}_m & \boldsymbol{\varphi}\boldsymbol{\varphi}^{\mathrm{T}} \\ \boldsymbol{\varphi}\boldsymbol{\varphi}^{\mathrm{T}} & \boldsymbol{I}_m \end{bmatrix}\boldsymbol{Q}^{\mathrm{T}} \tag{23}$$

$$\boldsymbol{\varphi} = \boldsymbol{L}_1^{-1}\boldsymbol{L}_2 \triangleq \left[\mu_{ij}\right], \boldsymbol{Q} = \begin{bmatrix} \boldsymbol{L}_1 & \boldsymbol{0} \\ \boldsymbol{0} & \boldsymbol{L}_1 \end{bmatrix} \tag{24}$$

Where, $\boldsymbol{I}_m$ is the unit matrix of m dimension. Since both $\boldsymbol{L}_1$ and $\boldsymbol{L}_2$ are lower triangular matrices, the matrix $\boldsymbol{\varphi}$ is also a lower triangular matrix. And,

$$\mu_{ii} = g_{ii}/b_{ii},\ i \in (1,\ m) \tag{25}$$

According to **Lemma 2**, if $b_{ii} \neq 0,\ i \in (1,\ m)$ is completely different from each other, the lower triangular matrix $\boldsymbol{L}_1$ can be diagonalized. Thus, its eigenvalue decomposition is recorded as:

$$\boldsymbol{L}_1 = \boldsymbol{P}_1\boldsymbol{\lambda}_1\boldsymbol{P}_1^{\mathrm{T}},\ \boldsymbol{\lambda}_1 \triangleq \mathrm{diag}\left(b_{ii}\right) \tag{26}$$

Similarly, the eigenvalue decomposition of the lower triangular matrix $\boldsymbol{\varphi}$ is recorded as:

$$\boldsymbol{\varphi} = \boldsymbol{P}_2\boldsymbol{\lambda}_2\boldsymbol{P}_2^{\mathrm{T}},\ \boldsymbol{\lambda}_2 \triangleq \mathrm{diag}\left(\mu_{ii}\right) \tag{27}$$

Definition :

$$\overline{\boldsymbol{P}}_1 \triangleq \begin{bmatrix} \boldsymbol{P}_1 & \boldsymbol{0} \\ \boldsymbol{0} & \boldsymbol{P}_1 \end{bmatrix},\ \overline{\boldsymbol{P}}_2 \triangleq \begin{bmatrix} \boldsymbol{P}_2 & \boldsymbol{0} \\ \boldsymbol{0} & \boldsymbol{P}_2 \end{bmatrix} \tag{28}$$

$$\boldsymbol{\tau} \triangleq \begin{bmatrix} \boldsymbol{\lambda}_1 & \boldsymbol{0} \\ \boldsymbol{0} & \boldsymbol{\lambda}_1 \end{bmatrix},\ \boldsymbol{\eta} \triangleq \begin{bmatrix} -\boldsymbol{I}_m & \boldsymbol{\lambda}_2^2 \\ \boldsymbol{\lambda}_2^2 & \boldsymbol{I}_m \end{bmatrix} \tag{29}$$

Based on the above eigenvalue decomposition, equation (23) can be further decomposed into:

$$\boldsymbol{y}_L = (\overline{\boldsymbol{P}}_1\boldsymbol{\tau}\overline{\boldsymbol{P}}_1^{\mathrm{T}})(\overline{\boldsymbol{P}}_2\boldsymbol{\eta}\overline{\boldsymbol{P}}_2^{\mathrm{T}})(\overline{\boldsymbol{P}}_1\boldsymbol{\tau}\overline{\boldsymbol{P}}_1^{\mathrm{T}}) \tag{30}$$

Hence,

$$\boldsymbol{y}_L^{-1} = (\overline{\boldsymbol{P}}_1\boldsymbol{\tau}^{-1}\overline{\boldsymbol{P}}_1^{\mathrm{T}})(\overline{\boldsymbol{P}}_2\boldsymbol{\eta}^{-1}\overline{\boldsymbol{P}}_2^{\mathrm{T}})(\overline{\boldsymbol{P}}_1\boldsymbol{\tau}^{-1}\overline{\boldsymbol{P}}_1^{\mathrm{T}}) \tag{31}$$

Therefore,

$$\begin{aligned} \rho(\boldsymbol{y}_L^{-1}\boldsymbol{Y}_{eq}) &\le \rho(\boldsymbol{y}_L^{-1})\rho(\boldsymbol{Y}_{eq}) \\ &\le \rho(\boldsymbol{\tau}^{-1})\rho(\boldsymbol{\eta}^{-1})\rho(\boldsymbol{\tau}^{-1})\rho(\boldsymbol{Y}_{eq}) \end{aligned} \tag{32}$$

Since both $\boldsymbol{\eta}$ and $\boldsymbol{Y}_{eq}$ are block diagonal matrices, the approximation based on formula (32) is as follows:

$$\begin{aligned} \rho(\boldsymbol{y}_L^{-1}\boldsymbol{Y}_{eq}) &\le \rho(\boldsymbol{y}_L^{-1})\rho(\boldsymbol{Y}_{eq}) \\ &\approx \rho\left(\mathrm{diag}(\sigma_k)\right) \end{aligned} \tag{33}$$

$$\sigma_k \triangleq \frac{\sqrt{\alpha_k^2+\beta_k^2}}{\sqrt{g_{kk}^4+b_{kk}^4}}, \quad k \in (1, \quad m) \tag{34}$$

σ_k, $k \in (1, \; m)$ in Formula (34) is the result of spectrum estimation. It has a direct physical correspondence with the load, that is, σ_k corresponds to the k load. Therefore, σ_k can be used to judge the voltage stability of the load node k. If $\sigma_k < 1$, it can be considered that the load is voltage stable; On the contrary, the voltage situation of the load is very "severe".

On the basis of the above, the load node voltage stability margin can be defined as follows:

$$\sigma_k^* \triangleq (1-\sigma_k)\times 100\%, \quad \sigma_k < 1 \tag{35}$$

When the grid topology is fixed, $\boldsymbol{y}_L$ is a constant matrix; when the grid topology changes, g_{kk}, b_{kk} $k \in (1, \; m)$ can be solved by one-time decomposition of $\boldsymbol{G}_L$ and $-\boldsymbol{B}_L$ by Cholesky decomposition. The amount of calculation is much less than that of eigenvalue decomposition. According to formula (17), (18), it is easy to realize on-line monitoring of α_k and β_k by using synchronous phasor measurement device PMU[17]. Therefore, under the existing conditions, it is easy to realize the real-time calculation and on-line monitoring of load node σ_k, $k \in (1, \; m)$.

Simulation Testing and Verification

In order to verify the effectiveness of the proposed method, a simulation test is carried out using the FDS program[11] developed by the Chinese Academy of Electrical Sciences, and the method is compared with the voltage stability analysis method based on Thévenin equivalence.

A 3-machine and 10-bus system[18] as shown in Figure. 2 is selected as an example system. The load at Bus 7 is set to 100% constant impedance load, and the load at Bus 10 is set to 80% induction motor load and 20% constant impedance load in parallel. The parameters of the induction motor for constant mechanical torque, stator impedance $\boldsymbol{Z}_1 = 0.01\text{+j}0.145$ pu, rotor impedance $\boldsymbol{Z}_2 = 0.008\text{+j}0.145$ pu, excitation reactance $\boldsymbol{X}_\mu = \text{j}3.3$ pu.

In the simulation test, a three-phase short-circuit fault occurred on the Bus 6 side of the tie-line between Bus 5 and Bus 6 at $t = 1.0$ seconds. The fault lasted 0.057 seconds and was cleared.

Figure 3 shows the power angle curve of the generator. Obviously, the generator power angle of the system is transient stable under the above fault conditions.

Figure 4 shows the voltage variation curve of the load node. Obviously, the load at Bus 10 is voltage unstable under the above fault conditions.

Figure 5 is the modulus tracking curve of Thévenin equivalent impedance and load equivalent impedance at Bus 10. Thévenin equivalent impedance is obtained directly by using the Thévenin equivalent parameter calculation program in FDS system. Obviously, if the impedance mode criterion based on Thévenin's equivalence is adopted, misjudgment will occur.

Figure 6 is a tracking monitoring curve of system voltage stability obtained directly from criterion (20). It can be seen from the diagram that no misjudgment will occur by using the method proposed in this paper. Compared with Figure 6 and Figure 5, it is obvious that the voltage stability criterion presented in this paper is more "sensitive" than the voltage stability criterion based on Thévenin equivalence.

Figure 7 is the result of tracking and monitoring the voltage stability of each load by σ_k. According to the voltage stability analysis method proposed in this paper, it is obvious that the load at Bus 10 is voltage unstable. It is easy to understand that the unstable load voltage at Bus 10 is the root cause of the unstable voltage of the whole system. From the comparison of Figure 7 and Figure 6, it can be seen that the difference between the monitoring results of load voltage stability at Bus 10 based on σ_k and that based on criterion (20) is very small, which shows that the calculation results of the spectrum method proposed in this paper are very close to those of the accurate eigenvalue method; in other words, the spectral calculation method proposed in this paper is similar to that of the eigenvalue method. It's more accurate.

To further test the effectiveness of the proposed method, based on the three-phase short-circuit fault mentioned above, 100 MW loads at Bus 10 are removed at s. Figure 8 shows the voltage amplitude curve of load node. Obviously, after partial load removal, the system voltage restores stability. Figure. 9 is the system voltage stability tracking monitoring result obtained by using criterion (20) directly. Figure. 10 is the load voltage stability tracking monitoring result based on. Obviously, using the method proposed in this paper, the voltage stability monitoring results can truly reflect the voltage stability of each load.

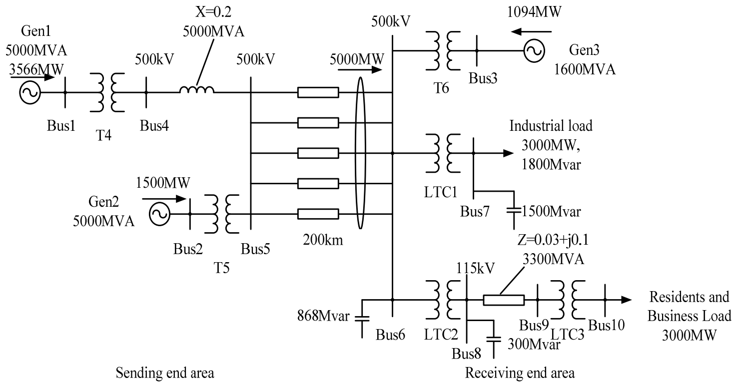

Figure 2. 3-machines and 10-bus system

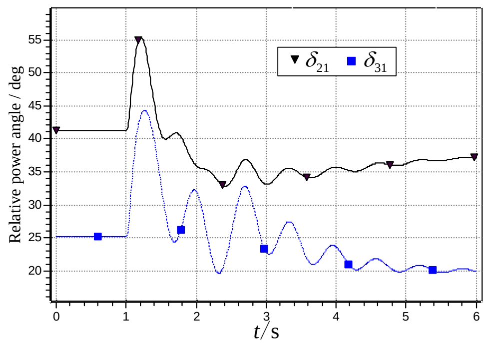

Figure 3. 3 Power angle curves of the machines

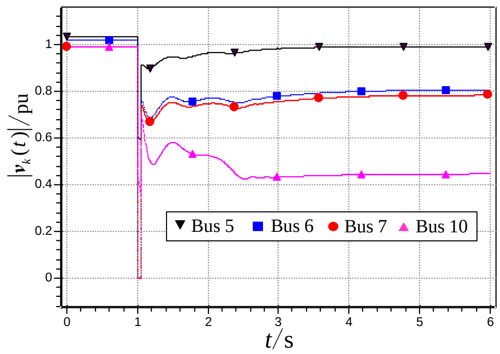

Figure 4. Load voltage curves

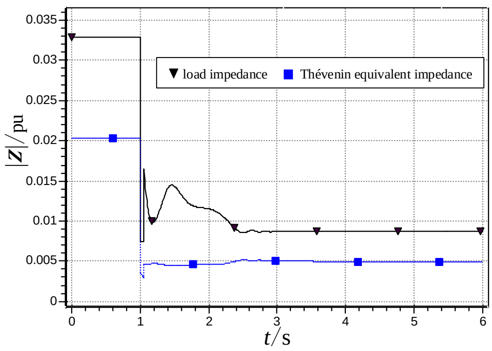

Figure 5. 3 Thévenin equivalent impedance and load impedance at Bus 10

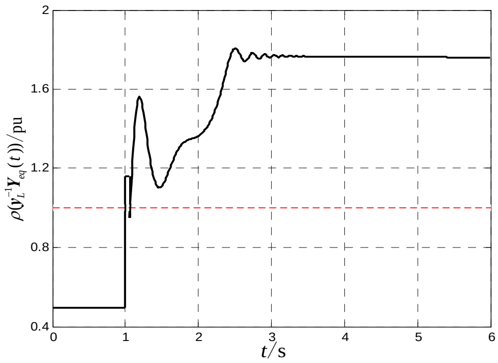

Figure 6. Voltage stability monitoring result for power system

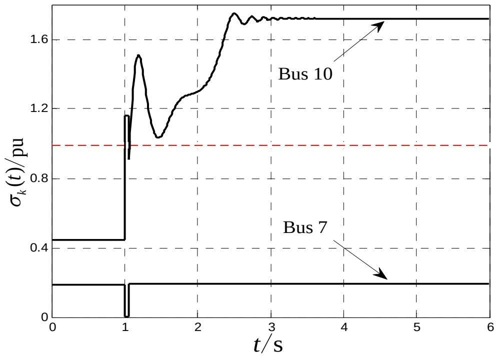

Figure 7. Load voltage stability monitoring result

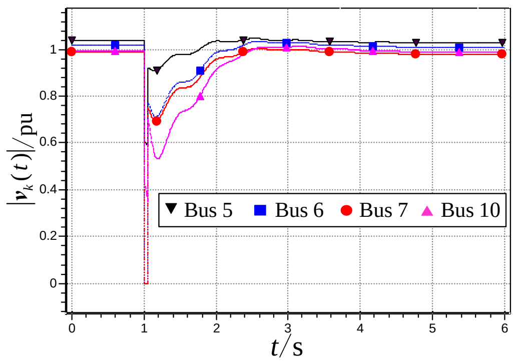

Figure 8. Load voltage curves after load shedding

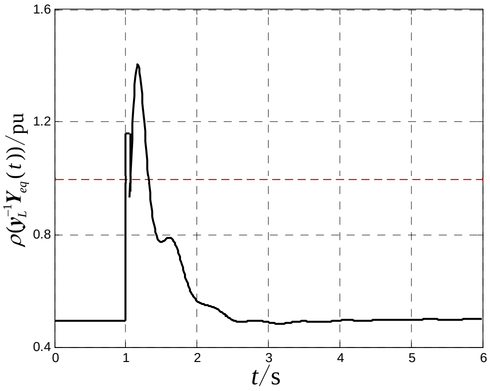

Figure 9. Voltage stability monitoring result for power system after load shedding

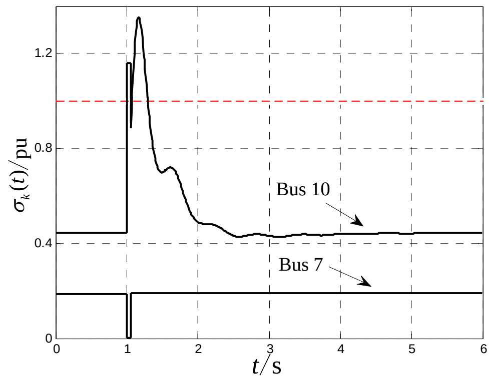

Figure 10. Load voltage stability monitoring result after load shedding

Conclusion

(1) Applying the fixed point theory to explain the voltage stability of the power system, the voltage stability analysis method based on the fixed point principle is proposed.

(2) In order to determine the physical correspondence between the spectrum distribution, i.e. the eigenvalue distribution and the specific loads, a corresponding and fast numerical method for estimating the spectrum distribution is derived, which establishes the relevant mathematical basis for the practicality of the voltage stability analysis method based on the fixed point principle.

(3) The proposed voltage stability analysis and calculation method has the advantages of less calculation and fast calculation and can be applied online. The simulation results preliminarily verify the effectiveness of the proposed method.

Acknowledgment

This work was supported by the projects of State Grid Corporation of China through its Grant XTB17201700252.

References

[1] P A Löf, T Smed, G Andersson, et al. Fast calculation of a voltage stability index[J]. IEEE Trans. on Power Systems, 1992, 7(1): 54-64.

[2] V Ajjarapu, C Christy. The continuation power flow: A tool for steady state voltage stability analysis[J]. IEEE Trans. on Power Systems, 1992, 7(1): 416-423.

[3] F Gubina, B Strmcnik. A simple approach to voltage stability assessment in radial networks[J]. IEEE Trans. on Power Systems, 1997, 12(3): 1121-1128.

[4] A C Z de Souza, C A Canizares, V H Quintana. New techniques to speed up voltage collapse computations using tangent vectors[J]. IEEE Trans. on Power Systems, 1997, 12(3): 1380-1387.

[5] T Van Cutsem, C Vournas. Voltage Stability of Electric Power System[M]. Boston: Kluwer Academic, 1998.

[6] Vu K, Begovic M, Novosel D, et al. Use of local measurements to estimate voltage-stability margin[J]. IEEE Trans. on Power Systems,1999,14(3):1029-1034.

[7] Y Wang, I R Pordanjani, W Li, et al. Voltage stability monitoring based on the concept of coupled single-port circuit[J]. IEEE Trans. on Power Systems, 2011, 26(4): 2154-2163.

[8] I R Pordanjani, Y Wang , W Xu. Identification of critical components for voltage stability assessment using channel components transform [J]. IEEE Trans. on Smart Grid, 2013, 4(2): 1122-1132.

[9] M Kamel, A A Karrar, A H Eltom. Development and application of a new voltage stability index for On-Line monitoring and shedding[J]. IEEE Trans. on Power Systems, 2018, 33(2): 1231-1241.

[10] Tang Yong, Sun Huadong, Yi Jun, et al. Tracing algorithm for Thevenin equivalent parameters based on complete differential equation[J]. Proceedings of the CSEE, 2009, 29(13): 48-53(in Chinese).

[11] Tang Yong, Yi Jun, Hou Junxian, et al. Calculation method for Thevenin equivalent parameters based on time domain simulation[J]. Proceedings of the CSEE, 2010, 30(34): 63-68(in Chinese) .

[12] Zhang Rui, Chen Shuyong, Liu Daowei, et al. Review of the Thévenin equivalent parameters identification methods[J]. Power System Technology, 2017, 41(1): 146-156(in Chinese).

[13] Tang Yong, Lin Weifang, Sun Huadong, et al. Method identifying voltage instability and angle instability based on tracking Thevenin equivalent parameters [J]. Proceeding of the CSEE, 2008, 29(25): 1-6(in Chinese).

[14] Li Weixing, Mou Xiaoming, Li Zhimin. Analysis and thoughts on the Thevenin equivalent parameters for power systems[J]. Proceeding of the CSEE, 2012, 32(S): 28-34(in Chinese).

[15] A Granas, J Dugundji. Fixed Point Theory[M]. New York: Springer-Verlag, 2003.

[16] Xu Zhong, Zhang Kaiyuan, Lu Quan, et al. A Brief Tutorial on Matrix Theory[M]. Beijing: Science Press,2005.

[17] B Milosevic, M Begovic. Voltage-stability protection and control using a wide-area network of phasor measurements[J]. IEEE Trans. on Power Systems, 2003, 18(1): 121-127.

[18] P Kundur, N J Balu, M G Lauby. Power System Stability and Control[M]. New York: McGraw-Hill Education, 1994.